Strain-Induced Crystallization Behavior of Polychloroprene Rubber

Peng Zhang, Guangsu Huang, Liangliang Qu, Yijing Nie, Gengsheng Weng, Jinrong Wu

College of Polymer Science and Engineering, State Key Laboratory of Polymer Material Engineering, Sichuan University, Chengdu 610065, China

Received 2 June 2010; accepted 11 October 2010
DOI 10.1002/app.33530
Published online 15 February 2011 in Wiley Online Library (wileyonlinelibrary.com).

ABSTRACT: The crystallization behavior of polychloroprene rubber (CR) has been studied in this work. Differential scanning calorimetry (DSC) was applied to characterize the crystallization behavior. And X-ray diffraction was applied to determine the impact of crosslinking on the crystallization of CR. Synchrotron X-ray diffraction (SXRD) method was applied to study the dynamic crystalline behavior. On the basis of the experimental results, it is found that crosslinking will hamper the crystallization of CR while large strain can restore this course. And this is in accord with the Mooney-Rivlin analysis result. Detailed discussion was offered circling around this phenomenon. © 2011 Wiley Periodicals, Inc. J Appl Polym Sci 121: 37–42, 2011

Key words: polychloroprene rubber; crystallization; strain induced crystallization; crosslinking

INTRODUCTION

Because of the poor crystalline nature of rubber materials, it has been a tricky problem to give a comprehensive study on the crystalline behavior of rubber even that calorimetry[1] and XRD[2] has long been applied to characterize the crystallization behavior. However, in recent years with the great progress of synchrotron X-ray diffraction (SXRD), it is possible to observe the crystalline behavior of rubber *in situ* due to the high diffraction intensity of synchrotron radiation. And lots of related studies have been reported.[2–7] Among them, the studies on natural rubber (NR) or its synthetic analog related studies have been most successful and explicit.[2–6] Besides, Toki et al.[7] have undertaken some primary study on general purpose synthetic rubbers such as butadiene rubber (BR), butyl rubber (IIR). However, to our best knowledge, the analogous work on comprehensive crystallization behavior of polychloroprene rubber (CR) combined with SXRD has not been undertaken yet.

It is well known that the stereochemical structures of CR and polyisoprene rubber (IR) are similar, but there is a significant difference in the conformation due to the replacement of methyl with chlorine which leads to different crystallization behavior. Moreover, CR has peculiar vulcanization behavior, which is concluded to ionic crosslinking.[8] So the study of CR crystallization will enrich the knowledge of rubber crystallization and offer more information on the effect of crosslinking on the crystallization behavior of rubber. And its application in the improving antifatigue properties of NR by blending NR and CR will be illustrated in our following works.

This work focuses on the impact of strain field, temperature, and crosslinking density variation on the crystallization of CR. To give a qualitative study, the SXRD was used to characterize the dynamical crystallization behavior during stretch and relax course; while X-ray diffraction with laboratory radiation source (XRD) and differential scanning calorimetry (DSC) were applied to study the impact of temperature and crosslinking density on the crystallization. Due to the limitation of the strain ratio during SXRD experiments, the stress–strain relation under universal testing machine was also determined to further explore the crystallization of CR based on the point of structure-property behavior.

EXPERIMENTAL DETAILS

Materials

Chloroprene (CR-2442, $\rho = 1.23$ g/cm^3, ML_{1+4} 100°C = 85, Changshou) which has fast crystalline ability is kindly supplied by Sichuan Rubber Factory, PRC.

Correspondence to: G. Huang (guangsu-huang@hotmail.com).

Contract grant sponsor: National Science Foundation of China; contract grant number: 50673059.
Contract grant sponsor: National Basic Research Program of China (973 Program); contract grant number: 2007CB714701.

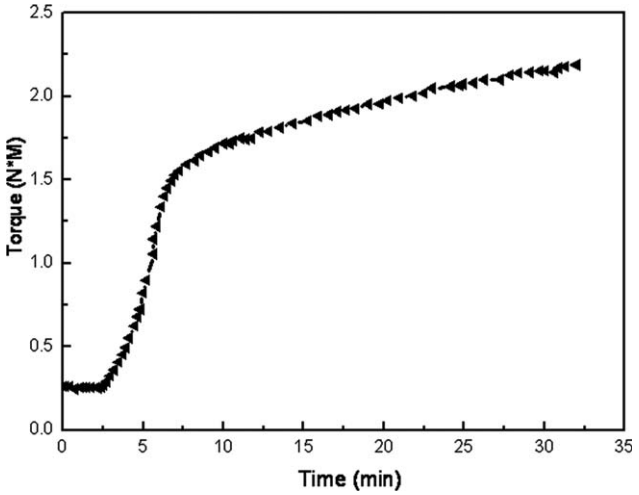

Figure 1 Curing curve of CR.

The accelerators used are *N*-Cyclohexyl -2-benzothiazyl sulfonamide (CZ) 0.5 phr and Diphenyl guanidine (DPG) 0.5 phr. Other compounding ingredients such as zinc oxide 5 phr, stearic acid 1.5 phr, magnesium oxide 4 phr and sulfur of commercial grades 0.5 phr are used without further purification. And the gum rubber was prepared with laboratory two-roll mill at room temperature and laid for at least 24 h for further test. The gum rubber was vulcanized at selected times at 150°C with hot-press.

Sample preparation

The sheeted rubber compound was conditioned at room temperature for 24 h before curing test using a Rheometer R 100E. The Rheometer gave outputs of curing curves as shown in Figure 1. From which, some curing parameters are achieved i.e., t_{10} (time required to achieve 10 Mooney units above the minimum viscosity), t_{50} (time required to achieve 50 Mooney units above the minimum viscosity), t_{90} (time required to achieve 90 Mooney units above the minimum viscosity). And serial samples of CR vulcanizate were prepared related to different cure times 4, 6, 20, and 45 min which corresponds to scorch time t_{10}, t_{50}, t_{90}, and fully vulcanized one, respectively. And to give a clear description for the sample with different cure times, S_n is applied to represent the sample with cure time n minutes.

Swelling experiment and crosslinking characterization

Toluene (AR, $\rho = 0.87$ g/cm^3) was chosen as the solvent and the vulcanizates with size of $7 \times 7 \times 2$ cm^3 were immerged in toluene for 24 h at room temperature. After equilibrium, the piece was wiped, evaporated, and weighed. And crosslink density was determined on the basis of the solvent-swelling measurements by application of the Flory-Rhener equation[9]

$$v_c = -\frac{\ln(1-v_2)+v_2+\chi v_2^2}{v_s\left(v_2^{\frac{1}{3}}-\frac{v_2}{2}\right)} \quad (1)$$

where v_2 is the volume fraction of CR in the swollen state; v_s is the molar volume of the solvent (106.2 for toluene) and the CR-toluene interaction parameter χ is 0.375.[10] The crosslinking results are shown in Table I. The statistic molecular weight between adjacent two crosslinks (M_c) was calculated with $M_c = \frac{1}{2V_c}$.[11]

Laboratory source radiation X-ray diffraction characterization

XRD patterns were collected on a Rigaku D/MAX-rA diffractomer with CuKα radiation ($\lambda = 1.5418$ Å), operating at 42 keV and 110 mA.

DSC characterization

Differential scanning calorimetry was performed on a thermal analyzer model in nitrogen atmosphere with a flow rate of 50 mL/min, using a DSC 204 (NETZSCH, Germany). The sample was set in an aluminum pan and cover. The dynamic procedure was undertaken as: first, cool the sample from room temperature to −20°C and equilibrated for 5 min; then, heat up the sample to 90°C at 10°C/min and equilibrated for 3 min; next, cools the sample to −20°C with 10°C/min; after another equilibrium at −20°C for 5 min, heat the sample to 90°C with 10°C/min.

Synchrotron radiation X-ray diffraction characterization

The width and thickness of X-ray samples were 1 mm and 1.5 mm, respectively, and the gauge length (length of the parallel part) was 5 mm. SXRD experiments were carried out at U7B beam-line in the National Synchrotron Radiation Laboratory (NSRL), University of Science and Technology of

TABLE I
Swelling Properties of CR Vulcanizate

Sample	W_2[a] (%)	V_2[b] (%)	V_C[c] ($\times 10^4$ mol/mL)	M_c[d] (g/mol)
S_4	0.20	0.15	0.83	6024
S_6	0.25	0.19	1.39	3597
S_{20}	0.25	0.19	1.41	3546
S_{45}	0.28	0.21	1.90	2631

[a] Weight fraction of CR.
[b] Volume fraction of CR.
[c] Crosslinking density.
[d] Statistic molecular weight between adjacent two crosslinks.

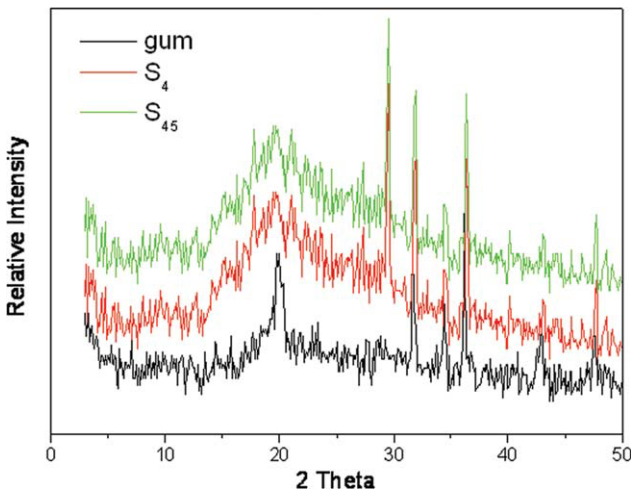

Figure 2 XRD patterns for CR gum and vulcanizates. [Color figure can be viewed in the online issue, which is available at wileyonlinelibrary.com.]

China, Hefei, P.R.C. The wavelength used in U7B was 0.154 nm.The two-dimensional (2D) XRD patterns were recorded in every 180 s by Mar CCD 165 X-ray detector system. To collect XRD patterns during deformation in real-time without holding the samples still, a homemade stretching machine with symmetric extension[4] is used at room temperature for deformation at strain rate of 4.2 mm/min. The Fit2D software package was used to analyze the 2D WAXD patterns. The work temperature was at 25°C.

Mechanical properties characterization

Tensile studies were performed using an Instron universal testing machine, Model 5576, according to ASTM D 412-87. No less than five pieces of each sample were tested and the average value was obtained. On the basis of the phenomenological theory of rubber elasticity, the Mooney-Rivlin equation was applied to deal with the stress–strain results and characterize the variation of modulus during stretch.[12]

RESULTS

Laboratory radiation source XRD characterization

The typical crystalline characteristics of CR gum and vulcanizate are shown as Figure 2. It is found that the CR gum shows sharp peaks at $2\theta = 20°$. And this is in accordance with the reflections of 200 and 120.[13,14] Whereas the S_4 and S_{45} present broad amorphous diffraction pattern around $2\theta = 20°$, which indicates that the vulcanization has obscured the crystallization of CR. When considering the other crystalline diffraction peaks, they are attributed to the diffraction features of metal oxides i.e., peak with $2\theta = 28°$ and 33° belong to ZnO (PDF Number 21-1486) and $2\theta = 37°$ belongs to MgO (PDF Number 65-0476).

DSC characterization

The concerning temperature induced crystallization (TIC) property of CR determined by DSC is shown in Figure 3. Figure 3(a) offers the heat flow variation of CR gum with temperature. Among which, there appears a sharp exothermic peak at −1.5°C in the first heating up course, indicating crystallization occurs, and then a broad rectangular endothermic peak appears between 25°C and 50°C which is attributed to the melting of crystals. Both the consecutive cooling and the second heating course, there is no dominant heat flow peaks, hence no detectable crystallization was observed. Comparative study on the S_4 is shown in Figure 3(b). After intensive observation, it is found that there is no peak lies in either heating up or cooling courses which implies that there is no detectable crystallization during the DSC experiment.

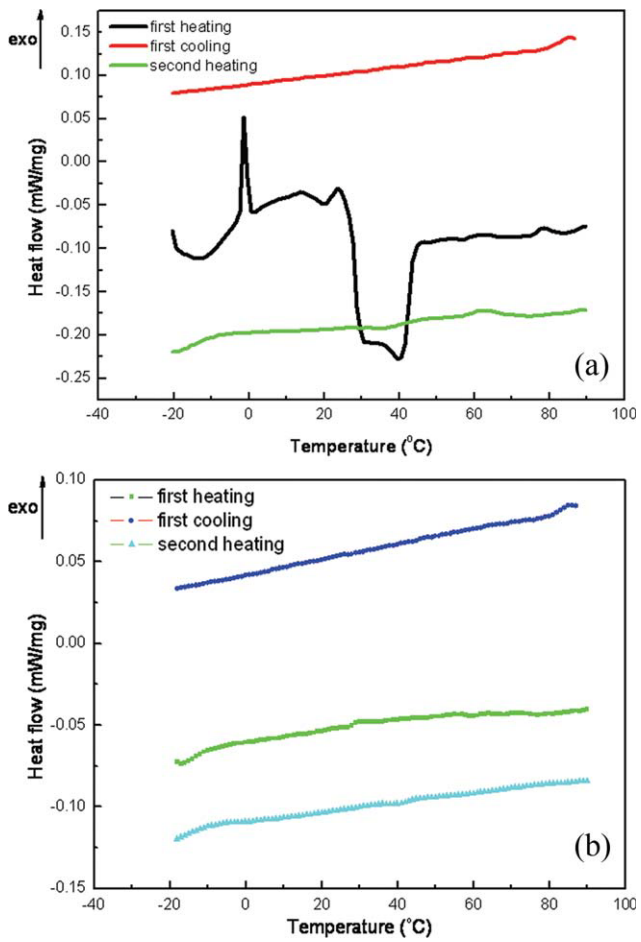

Figure 3 DSC curves of CR gum (a) and vulcanizate cured for 4 min i.e., S_4 (b). [Color figure can be viewed in the online issue, which is available at wileyonlinelibrary.com.]

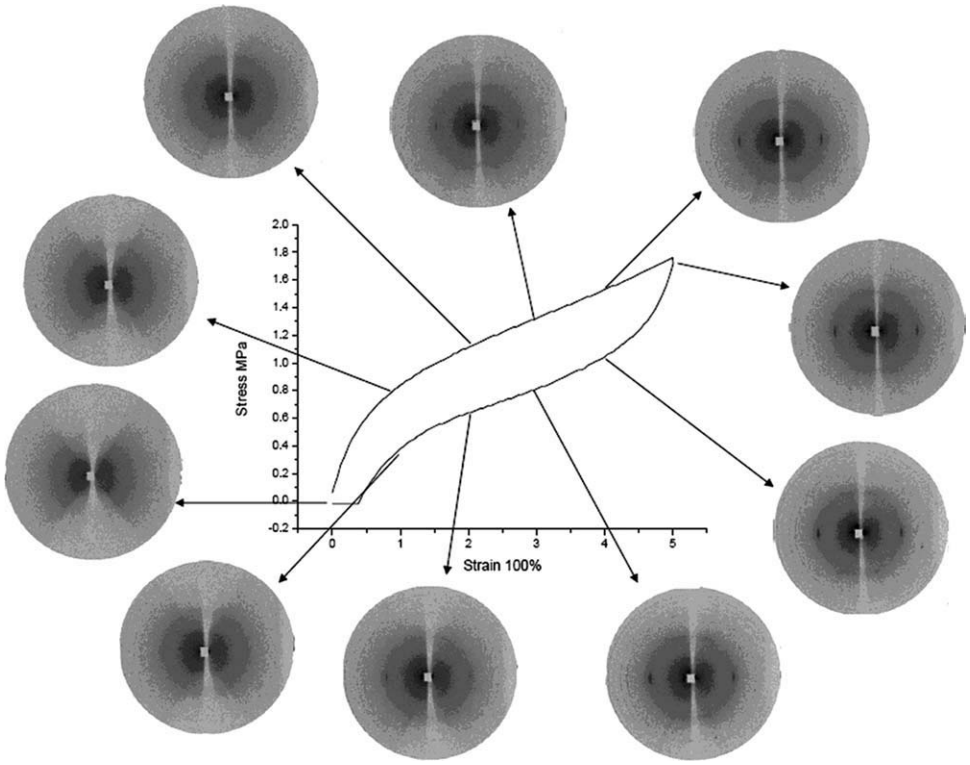

Figure 4 SXRD patterns for CR during stretch and relaxation.

SXRD characterization

The stress–strain curve of S_{45} and the typical changes in SXRD patterns of the sample during the stretching and retraction are shown in Figure 4. And the arrow lines link the determined SXRD pattern and the approximate elongation ratio. As shown in the stress-strain curve, a linear increment of the stress with the variation of strain is observed in the stretching process after α exceeds ~ 1. When the retraction concerned, the stress decreased abruptly at the beginning. And the correlated SXRD patterns show that there is no observable crystalline feature in the unstretched state and the faint crystallization reflections appear at $\alpha = 3$ and proceeds slowly with the strain during stretch; under retraction, the crystallization reflection retains at first and then diminishes till $\alpha = 1$ disappears.

Mechanical properties

Typical stress versus strain curves of CR are shown in Figure 5(a). For all four curves, there are stress upturns at α no less than 4. Some interesting works based on the elastic network nature of rubber were undertaken by plotting the reduced stress σ^* [$\sigma^* = \sigma/(\alpha - \alpha^{-2})$] against the reciprocal of the extension ratio α (where σ is the nominal stress defined as the force divided by the undeformed cross-sectional area and α is the extension ratio)[12] as shown in Figure 5(b). This representation is suggested by the Mooney-Rivlin equation[15]

$$\sigma* = 2C_1 + 2C_2\alpha^{-1} \tag{2}$$

where C_1 and C_2 are constants independent of α. It is observed that there is an abrupt depression of σ^* at $\alpha^{-1} = 0.21$ which corresponds to $\alpha = 4.76$. This is due to the self-toughing of CR from crystallization.

DISCUSSION

It has been well recognized that CR-2442 is able to crystallize due to the high regularity of molecule structure and *trans*-conformation segments take main part in crystallization.[13,16–18] And this is verified by the XRD and DSC experiment results of CR gum in our work i.e., the sharp XRD reflection peak at $2\theta = 20^\circ$ and large endothermic peak during DSC first heating. Hence the addition of vulcanizing agents will not change the crystalline behavior of CR until vulcanization occurs. However, from the viewpoint of structure-property relationship, it's important to detect the crystal melt and restoration behavior with the variation of crosslinking degree. As shown in Figure 3(a), for the first heating course, the crystallites melting peaks is bigger than that of the crystalline one. This means that the crystallization of CR gum mainly comes from the room temperature

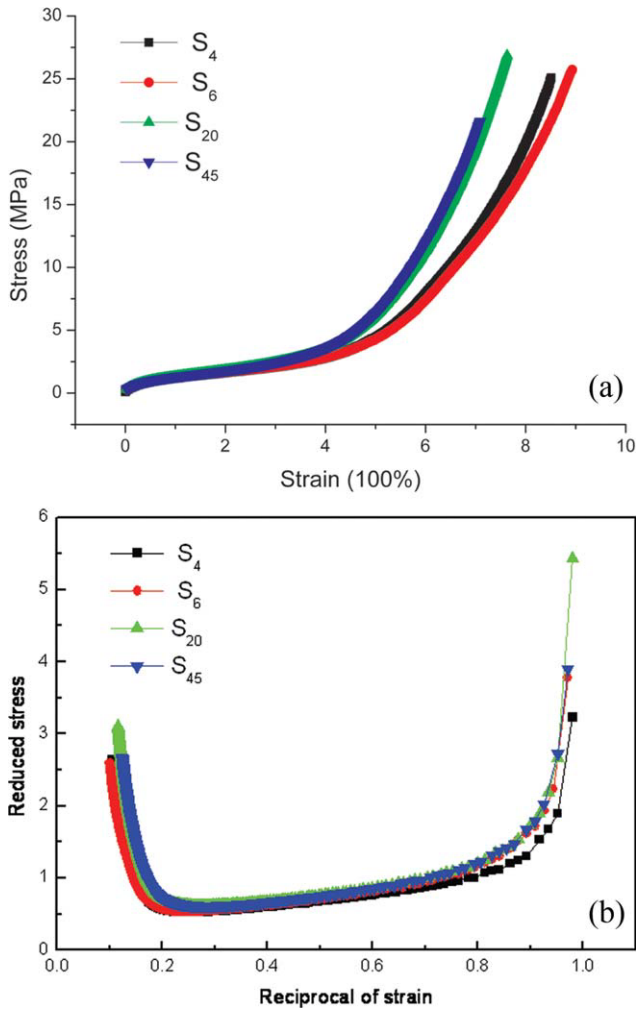

Figure 5 Stress-strain curves (a) and Mooney- Rivlin plots (b) for CR vulcanizates (S_n is applied to represent the sample with cure time n minutes). [Color figure can be viewed in the online issue, which is available at wileyonlinelibrary.com.]

storage before test except for the sharp exothermic peak at −1.5°C which shows crystallites grows during the first heating course. In the following part, we have undertaken the consecutive cooling, isothermal and heating courses of DSC experiment, among which the crystallization has not been observed. It should be mentioned that the crystal nucleus disappears after isothermal heating at 90°C. And the crystal nucleation and growth theory is taken into consideration to explain this phenomenon. Nucleation is a bulk property of material and is found to greatly temperature-related because the nucleation step is an activated process which needs to surmount a free energy barrier.[18,19] If only the crystallization behavior of CR gum is focused on, the disappearance of detectable crystallization trace in DSC cooling and second heating experiments is due to the fast cooling or heating rate which is much lower than the necessary crystal nucleation time. For example, the maximum rate of crystallization of CR-2442 is around −5°C and the corresponding $t_{1/2}$ (determined by time to reach half the limiting degree of crystallization) is 0.77 h.[20] Hence there is no detectable crystal nucleus appear and grow in the following cooling or heating. And this is the reflection of the time-related nature of CR crystallization.[18,21] While taking the CR vulcanizate into consideration, there is no detectable crystallization during experiment. Considering the lower limitation of equipments, e.g., the reported lower limits of XRD detection of single crystal is on the order of 100 μm^3, depending on the composition and X-ray beam condition,[22] this is also attributed to the fact that the dense crosslinks have hampered the molecular mobility of CR. It is reported that the dehydrohalogenation induced reactions, e.g., the formation of C=C or C=O, do not have any effect on the rate of nucleation or the growth of crystallization centers until crosslinking hampers the mobility of neighboring segments.[23] As shown in Table I, the calculated M_c (statistic molecular weight between adjacent two crosslinks) of S_4 is 6024 g/mol which correspond to about 68 repeating units of CR. Further analysis is based on the hard invasion of crosslinks in more regular *trans*-CR zones, hence the amorphous zones of CR is more densely crosslinked, namely, the crystalline *trans*-CR molecular segments are surrounded by densely crosslinked amorphous zones of CR. In conclusion, the crosslinking and its uneven distribution hampered the crystallization of CR vulcanizate during room temperature storage.

To further explore the crystallization behavior of CR-2442, it's naturally to take the strain-induced crystallization (SIC) into consideration and SXRD is one of the most powerful tools. As shown in Figure 4, the undrawn S_{45} shows no crystalline feature but a large dark zone surrounding the core which indicates that most rubber molecules are amorphous. This is in accordance with the XRD results of S_{45}. And the difference is that there appear crystalline spots at the equator of the diffraction pattern with the proceeding of strain which indicates that the CR vulcanizate restores the crystalline feature under the function of stress field. Besides, the amorphous dark zone exists in either diffraction pattern during stretching or relaxation indicates that most CR is amorphous. Considering the fact that large strain will lead to enhancement of supercooling,[21,24] it's reasonable to infer that high strains can offer more supercooling degree to promote the crystallization of CR. Moreover, as illustrated above, the increase of curing time will definitely cut down the space of *trans*-CR and less crystallization occurs. So the crystalline feature of CR vulcanizate is not as clear as that of IR or NR.[7,25] Consequently, the calculation

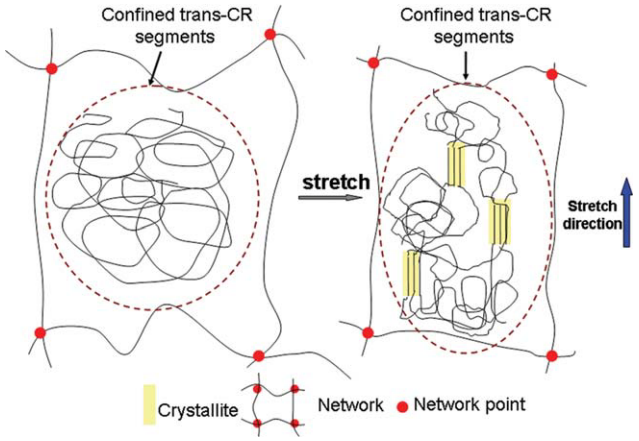

Figure 6 Schematic model of deformed CR vulcanizate: undeformed networks and deformed networks (which consists of oriented crystallites, crosslinking points, and nominal crosslinking network). [Color figure can be viewed in the online issue, which is available at wileyonlinelibrary.com.]

of the crystalline degree based on SXRD results is considered incredible here. As supplementary, the exploration of the crystallization at large strain was undertaken with Universal tensile tester and the Mooney-Rivlin analysis.

The tensile curves are shown in Figure 5(a). According to which, there are dominant stress upturns which are usually treated as the result of SIC in semicrystalline polymers, i.e., NR, IR[26] and CR in the range of $\alpha > 400\%$. Because of the restriction of lower detect limit, this value is larger than that of more accurate SXRD results. Moreover, as shown in Figure 5(b), there is a large and abrupt increase of reduced modulus when the extension ratio exceeds about 476%. This phenomenon has been illustrated to the self-toughing of crystals.[12] So the variation of the crosslinked network under large strains has promotes the orientation of *trans*-CR segments and crystallization occurs. On the basis of the above results and discussion, the schematic variation of the restricted crystallization of CR is offered in Figure 6. In the diagram, the nominal network indicates the surrounding amorphous CR molecules which take active part in crosslinking; the crystallites indicate the regularly arranged part of molecules. As sketched in the picture, when the external force is exerted on the sample the crosslinking network deforms and changes the molecular conformations which finally lead to SIC.

CONCLUSION

The study focuses on the crystallization behavior of CR has been undertaken in this work. The XRD and DSC experiments have proved that CR gum has strong TIC ability except that crosslinking will greatly hamper this course. This is related to the fact that the melting of the crystalline nucleus and the restoration is a time-consumed course under sole temperature field and crosslinking restricts the crystalline nucleation course of CR by restricting the mobility of *trans*-conformation parts. Furthermore, it has been found that the CR vulcanizates as prepared in this work show faint SIC feature when the strain ratio is above 300%. By further certification with tensile modulus variation and Mooney-Rivlin analysis, we supposed the schematic crystallization course of CR vulcanizate under large strain as shown in Figure 6.

The authors thank Dr. Liangbin Li and Dr. Guoqiang Pan of National Synchrotron Radiation Laboratory (NSRL) in University of Science and Technology of China for their kindly help in Synchrotron WAXD experiments.

References

1. Woodand, L. A.; Bekkedahl, N. J Appl Phys 1946, 17, 362.
2. Toki, S.; Hsiao, B. S.; Amnuaypornsriand, S.; Sakdapipanich, J. Polymer 2009, 50, 2142.
3. Tosaka, M. Macromolecules 2009, 42, 6166.
4. Qu, L. L.; Huang, G. S.; Liu, Z. Y.; Zhang, P.; Wengand G. S.; Nie, Y. J. Acta Materialia 2009, 57, 5053.
5. Carretero-Gonzalez, J.; Verdejo, R.; Giannelis, E. P.; Toki, S.; Hsiaoand, B. S.; Lopez-Manchado, M. A. Macromolecules 2008, 41, 2295.
6. Amnuaypornsri, S.; Sakdapipanich, J.; Toki, S.; Hsiao, B. S.; Ichikawaand, N.; Tanaka, Y. Rubber Chem Technol 2008, 81, 753.
7. Tokiand, S.; Hsiao, B. S. Macromolecules 2003, 36, 5915.
8. Desai, H.; Hendrikseand, K. G.; Woolard, C. D. J Appl Polym Sci 2007, 105, 865.
9. Flory, P. J. Principles of Polymer Chemistry; Cornell University Press: Ithaca, NY, 1953; p 576.
10. Brandrup, J.; Immergut, E. H.; Grulke, E. A. Polymer Handbook; Wiley-Interscience Publication: New York, 1999.
11. Naunton, W. J. S. Applied Science of Rubber; Edward Arnold Press: London, 1961.
12. Joly, S.; Garnaud, G.; Ollitrault, R.; Bokobzaand, L.; Mark, J. E. Chemistry of Materials 2002, 14, 4202.
13. Krigbaumand, W. R.; Roe, R. J. J Polym Sci Part A-General Papers 1964, 2, 4391.
14. Riva, F.; Forteand, A.; Dellamonica, C. Colloid Polym Sci 1981, 259, 606.
15. Erman, B.; Mark, J. E. Structures and Properties of Rubber Like Networks; Oxford University Press: New York, 1997.
16. Davies, C. K. L.; Long, O. E. J Mater Sci 1977, 12, 2165.
17. Tsuji, M.; Shimizuand, T.; Kohjiya, S. Polymer J 1999, 31, 784.
18. Tsuji, M.; Shimizuand, T.; Kohjiya, S. Polymer J 2000, 32, 505.
19. Gibson, J. M. Science 2009, 326, 942.
20. Li, P.; Zhou, S. Y. China Synthetic Rubber Industry 1987, 10, 364.
21. Aligand, I.; Tadjbakhsch, S. J Polym Sci Part B-Polym Phys 1998, 36, 2949.
22. Pluth, J. J.; Smith, J. V.; Pushcharovsky, D. Y.; Semenov, E. I.; Bram, A.; Riekel, C.; Weberand, H. P.; Broach, R. W. Proc Natl Acad Sci USA 1997, 94, 12263.
23. Kösslerand, I.; Scaronvob, L. J Polym Sci 1961, 54, 17.
24. Tosaka, M.; Murakami, S.; Poompradub, S.; Kohjiya, S.; Ikeda, Y.; Toki, S.; Sicsand, I.; Hsiao, B. S. Macromolecules 2004, 37, 3299.
25. Trabelsi, S.; Albouyand, P. A.; Rault, J. Macromolecules 2003, 36, 7624.
26. Tosaka, M.; Kawakami, D.; Senoo, K.; Kohjiya, S.; Ikeda, Y.; Tokiand, S.; Hsiao, B. S. Macromolecules 2006, 39, 6784.